

Gel to glass transition in simulation of a valence-limited colloidal system

E. Zaccarelli,^{1,2} I. Saika-Voivod,^{3,4} S. V. Buldyrev,⁵ A. J. Moreno,^{6,7} P. Tartaglia,⁶ and F. Sciortino¹

¹ *Dipartimento di Fisica and CNR-INFM-SOFT,
Università di Roma 'La Sapienza', P.le A. Moro 2, I-00185, Roma, Italy*

² *ISC-CNR, Via dei Taurini 19, I-00185, Roma, Italy*

³ *Department of Chemistry, University of Saskatchewan, Saskatoon, Saskatchewan, S7N 5C9*

⁴ *Dipartimento di Fisica, Università di Roma 'La Sapienza', P.le Aldo Moro 2, I-00185, Roma, Italy*

⁵ *Yeshiva University, Department of Physics, 500 W 185th Street New York, NY 10033, USA*

⁶ *Dipartimento di Fisica and CNR-INFM-SMC, Università di Roma 'La Sapienza', P.le A. Moro 2, I-00185, Roma, Italy*

⁷ *Donostia International Physics Center, Paseo Manuel de Lardizabal 4, E-20018 San Sebastián, Spain*

(Dated: July 9, 2021)

We numerically study a simple model for thermo-reversible colloidal gelation in which particles can form reversible bonds with a predefined maximum number of neighbors. We focus on three and four maximally coordinated particles, since in these two cases the low valency makes it possible to probe, in equilibrium, slow dynamics down to very low temperatures T . By studying a large region of T and packing fraction ϕ we are able to estimate both the location of the liquid-gas phase separation spinodal and the locus of dynamic arrest, where the system is trapped in a disordered non-ergodic state. We find that there are two distinct arrest lines for the system: a *glass* line at high packing fraction, and a *gel* line at low ϕ and T . The former is rather vertical (ϕ -controlled), while the latter is rather horizontal (T -controlled) in the $(\phi - T)$ plane. Dynamics on approaching the glass line along isotherms exhibit a power-law dependence on ϕ , while dynamics along isochores follow an activated (Arrhenius) dependence. The gel has clearly distinct properties from those of both a repulsive and an attractive glass. A gel to glass crossover occurs in a fairly narrow range in ϕ along low T isotherms, seen most strikingly in the behavior of the non-ergodicity factor. Interestingly, we detect the presence of anomalous dynamics, such as subdiffusive behavior for the mean squared displacement and logarithmic decay for the density correlation functions in the region where the gel dynamics interferes with the glass dynamics.

PACS numbers: 82.70.Gg, 82.70.Dd, 64.70.Pf

I. INTRODUCTION

Systems composed of mesoscopic solid particles dispersed in a fluid are named colloids. The properties of the particles and of the fluid can be controlled via chemical or physical manipulations to a great extent. As a result the particle-particle interaction can be tuned from very short range depletion attractions to very long range Coulombic repulsion [1], making colloids important both in terms of basic scientific research and industrial applications [2, 3, 4, 5]. The canonical model system for colloids is the hard sphere system, for which sterically stabilized colloidal particles such as PMMA provide a very accurate experimental realization [6, 7]. Hard sphere colloids have been used to directly observe crystal nucleation and to test theoretical predictions surrounding glass transitions[8]. The addition of small, non-adsorbing polymers to a hard-sphere solution leads to a short-range effective attraction between colloids through the so-called depletion interaction [9, 10]. The size of the small polymer controls the range of attraction, while the concentration controls the strength of attraction u_0 . Neglecting the role of solvent interactions, these systems can be simulated on a computer with a short-range attractive potential, as simple as a hard core complemented by a square well (SW). Colloid-polymer mixtures have been found to offer new scenarios of arrested states. These hard sphere plus short range attraction

systems exhibit the usual hard sphere glassy dynamics near $\phi \approx 0.6$. However, a fascinating phenomenon arises when the range of attraction is less than approximately 10% of the hard sphere diameter, that is a re-entrance of the glass transition line, predicted by Mode Coupling Theory (MCT) [11, 12, 13], and confirmed by several experiments[14, 15, 16, 17, 18, 19] and simulations [20, 21, 22, 23, 24]. In this case, for a particular range of ϕ , arrest can be achieved by either increasing or decreasing T/u_0 , the ratio of temperature T to attraction strength u_0 . The two types of glass are now commonly named hard-sphere or repulsive glass for the one at higher T , and attractive glass for the one at lower T .

At low densities short-range attractive colloids exhibit particle clustering and gelation[25, 26, 27, 28]. Recently, several numerical works have focused on colloidal gelation [29, 30, 31, 32, 33, 34], with the aim of better characterizing colloidal gels and attempting to formally connect gel to glass formation [12, 26, 30, 35, 36]. Following MCT ideas, the gel state was interpreted as a low ϕ extension of the high ϕ attractive glass [12, 35, 36, 37] and, generating some confusion, the term "gel" is still often interchanged with the term 'attractive glass'.

Differently from chemical gelation, that was extensively studied in polymer physics[38, 39, 40] and modeled in computer simulations[41, 42, 43, 44, 45, 46], colloidal gelation is still quite poorly understood. Gelation arises when a stable particle network is formed due to

bonding. For chemical gels, bonds are irreversible, and thus gelation can be explained in terms of percolation theory. However, the bonds intervening in colloidal aggregation have an energy typically of the order of $k_B T$, as for example bonds induced by depletion interactions. Thus such bonds are mostly transient at finite attraction strength. The existence of a finite bond lifetime creates a gap between the location of the percolation line and the dynamic arrest (gel) line. Earlier simulations on a lattice[41, 45, 47] and off-lattice[46] have discussed the influence of reversible bond formation on the gelation process.

The quest for bond stabilization often calls for exploring regions of very high attraction strength in the phase diagram to increase the bond lifetime and promote gelation. However, in this region, at low packing fraction ϕ and at low T (or at high u_0 values), a phase separation into gas (colloid-poor) and liquid (colloid-rich) always takes place[48]. Recent theoretical studies have addressed the question of the relative location of the phase separation and of the attractive glass line. It has been found[49, 50] that the attractive glass line meets the spinodal at a finite temperature, on the high density side. At low ϕ , arrest in (spherically interacting) short-range attractive colloids occurs only as arrested phase separation, where the liquid phase is glassy, and hence the phase separation cannot proceed fully [49]. This scenario was found in numerical simulations of the square well potential for a well width ranging from 15% to arbitrarily small values[49, 50, 51], as well as in Lennard-Jones potential[52]. Gels as a result of interrupted phase separation have been identified in experiments[53] and simulations[49, 54, 55]. For extremely deep quenches (at very low T) irreversible gelation may occur through diffusion limited cluster aggregation [56, 57, 58, 59, 60].

Other mechanisms must be invoked for stabilization of thermo-reversible gels and suppression of the spinodal line[61]. A possibility is to consider the effect of residual charges on the colloidal particles, that may produce a long-range repulsive barrier in the interparticle potential, thus efficiently stabilizing the bonds and preventing the condensation of the liquid phase. The emergence of an equilibrium cluster phase has been recently evidenced both in experiments[62, 63] and simulations[30, 31, 32] on charged colloidal and protein suspensions. A dynamical arrest transition then follows, driven by electrostatic repulsions between the clusters [30] or by cluster branching and percolation [31, 32].

Very recently, forming a gel *in equilibrium*, without the interference of phase separation, has been achieved by limiting the number of attractive interactions (bonds) between nearest neighbors. Following ideas first introduced by Speedy and Debenedetti [64, 65], a model for thermo-reversible gelation has been studied numerically[33]. This model, in which particles interact via a SW potential with the addition of a geometrical constraint in the maximum number of bonds n_{\max} a particle can form, describes particles interacting via a hard-core plus n_{\max}

randomly-located sticky spots[66]. In this respect, the model retains the spherical symmetry but incorporates features of associating liquids[67]. Other possibilities to limit the number of bonded pairs implementing geometrical constraints and retaining a spherical pair potential can be found in Ref.[68, 69], while the same basic ideas have inspired recent work on self-assembly of super-molecular/nano structures [70, 71]. In the literature it is possible to find several related models, also based on limited short-range attractions in which the bonding constraint is imposed via angular degrees of freedom, though the focus has not always been on their dynamic properties[34, 72, 73, 74, 75]. In general, ref [33] puts forward the hypothesis that, only when a restricted part of the colloidal surface is active in the formation of attractive bonds, dynamic arrest at low ϕ can be observed in the absence of a phase separation. An experimental test of the previous hypothesis will hopefully be provided by the new generation of ‘patchy’ colloids, or colloids with ‘sticky spots’ [76], which is about to be synthesized.

Understanding gelation at low densities in short-range attractive models may also be relevant to the study of proteins, since they are expected to belong to the class of short-range attractive interacting systems[73, 77]. Indeed, the formation of arrested disordered states at low densities often interferes with crystallization, and this is possibly one of the reasons why proteins are often difficult to crystallize [78, 79].

In a recent Letter [33], we showed that the n_{\max} model (detailed in section II below) allows us to study thermo-reversible gels. We showed that the signatures of the gel state, as for example the non-ergodicity factor f_q , are quite distinct from those of both the hard sphere and the attractive glass. In the present study, we explore the full- ϕ dependence of dynamics at low T for both $n_{\max} = 3$ and $n_{\max} = 4$. We observe a transition over a small range in ϕ from a gel to a repulsive glass. In Section II, we give details of the model and simulations. Section III contains the results for the calculated phase diagram and compares the relative location of the thermodynamic and of the kinetic arrest lines. We also report static and dynamic correlation functions. In Section IV we discuss results and in Section V conclusions are drawn.

II. SIMULATION DETAILS

We perform event-driven molecular dynamics simulations of $N = 10000$ particles of mass $m = 1$ with diameter $\sigma = 1$ (setting the unit of length) interacting via a limited-valency square well potential. The depth of the well u_0 is fixed to 1, and the width Δ of the square well attraction is such that $\Delta/(\sigma + \Delta) = 0.03$. T is measured in units of u_0 , and the unit of time t is $\sigma(m/u_0)^{1/2}$. This system is a one-component version of the binary mixture that has been extensively studied previously [22, 49, 80, 81]. In the following we will use the acronym SW to indicate the $\Delta/(\sigma + \Delta) = 0.03$ standard

square well potential. The limited-valency condition is imposed by adding a bonding constraint. The square well form can be used to unambiguously define bonded particles, i.e., particles with centers lying within σ and $\sigma + \Delta$ of each other are bonded. The interaction between two particles i, j , each having less than n_{\max} bonds to other particles, or between two particles already bonded to each other, is thus given by a square-well potential,

$$V_{ij}(r) = \begin{cases} \infty & r < \sigma \\ -u_0 & \sigma < r < \Delta \\ 0 & r > \sigma + \Delta. \end{cases} \quad (1)$$

When i and/or j are already bonded to n_{\max} neighbors, then $V_{ij}(r)$ is simply a hard sphere (HS) interaction,

$$V_{ij}(r) = \begin{cases} \infty & r < \sigma \\ 0 & r > \sigma. \end{cases} \quad (2)$$

The resulting Hamiltonian of the system has a many-body term containing information of the existing bonds. Due to the fact that the list of existing bonds is necessary at any instant of the simulation, configurations are saved storing also the bond list. Moreover, all simulations are started from high temperature configurations where all particle overlaps are excluded within the attractive well distance $\sigma + \Delta$. In cases of multiplicity of possible bondings, such as for example when a bond is broken for a particle that was fulfilling the n_{\max} allowed bonds and more than one neighbour particle lie within its attractive well, a random neighbour, with less than n_{\max} bonds, is chosen to form the new bond.

The idea of constraining the number of square well bonds a particle can form was introduced by Speedy and Debenedetti [64, 65]. In contrast to their original version of the model, where triangular closed loops were not allowed, in the present model no constraints on minimal bonded loops are introduced. Our model can be considered as a realization of particles with n_{\max} randomly located ‘sticky spots’[66]. The limited-valency properly defines the ground state of the systems, corresponding to a potential energy per particle $-u_0 n_{\max}/2$. This is achieved when every particle has n_{\max} filled bonds. We note that fully bonded clusters of finite size may occur. The smallest fully connected cluster sizes are: 4 (tetrahedra) for $n_{\max} = 3$; 6 (octahedra) for $n_{\max} = 4$; and 12 (icosahedra) for $n_{\max} = 5$. This introduces the intriguing possibility of forming a hard sphere gas of such clusters at low ϕ and T , as seen from the simulations. We study in depth the cases $n_{\max} = 3$ and 4, for which we already know that there exist significant differences in the location of the spinodal lines as compared to the $n_{\max} = 12$ (or standard SW) case.

For all state points simulated, we first equilibrate the system at constant T until the potential energy and pressure of the system reach a steady state, and the MSD reaches diffusive behavior, i.e., during the equilibration

time particles move on average at least one particle diameter. A subsequent constant energy simulation is used to gather statistics for all reported quantities.

To estimate the equilibrium phase diagram, we calculate the gas-liquid spinodal and the static percolation line. The latter is defined as the locus in (ϕ, T) such that 50% of the configurations possess a spanning, or percolating, cluster of bonded particles. To characterize the structure and dynamics of the system, we evaluate: the static structure factor,

$$S(q) \equiv \langle |\rho_q(0)|^2 \rangle, \quad (3)$$

the mean squared displacement (MSD),

$$\langle r^2(t) \rangle \equiv \langle \sum_{i=1}^N |\vec{r}_i(t) - \vec{r}_i(0)|^2 / N \rangle, \quad (4)$$

the diffusion coefficient,

$$D \equiv \lim_{t \rightarrow \infty} \left\langle \sum_{i=1}^N |\vec{r}_i(t) - \vec{r}_i(0)|^2 \right\rangle / 6Nt, \quad (5)$$

the dynamic structure factor, or density autocorrelation function,

$$F_q(t) \equiv \langle \rho_q(t) \rho_{-q}(0) \rangle / \langle \rho_q(0) \rho_{-q}(0) \rangle, \quad (6)$$

and its long time limit or plateau value f_q , i.e. the non-ergodicity parameter. In all cases, $\langle \cdot \rangle$ denotes an ensemble average, \vec{r}_i is the position vector of a particle, \vec{q} is a wavevector and i labels the N particles of the system, while $\rho_q(t) = \frac{1}{\sqrt{N}} \sum_{i=1}^N \exp(-i\vec{q} \cdot \vec{r}_i)$.

Also, we monitor the bond lifetime correlation function, averaged over different starting times, and defined as,

$$\phi_B(t) = \langle \sum_{i < j} n_{ij}(t) n_{ij}(0) \rangle / [N_B(0)], \quad (7)$$

where $n_{ij}(t)$ is 1 if two particles are bonded up to time t and 0 otherwise, while $N_B(0) \equiv \langle \sum_{i < j} n_{ij}(0) \rangle$ is the number of bonds at $t = 0$. We note that ϕ_B counts which fraction of bonds found at time $t = 0$ persists at time t , without ever breaking within the store rate of configurations. Associated with $\phi_B(t)$, we extract an estimate of the bond lifetime τ_B via stretched exponential fits.

Although colloidal systems are more properly modeled using Brownian dynamics, we use event driven molecular dynamics due to its efficiency in the case of step-wise potentials. While the short-time dynamics is strongly affected by the choice of the microscopic dynamics, the long term structural phenomena, in particular close to dynamical arrest, are rather insensitive to the microscopic dynamics [75, 82]. To have a confirmation of this, we also performed additional simulations where the effect of the solvent was mimicked by so-called ghost particles [83].

In particular, we studied a system of 1000 colloidal particles and 10000 ghost particles and we found that the long-time behavior of the dynamical quantities, such as the T dependence of τ_B and the q dependence of f_q are independent from the microscopic dynamics. We also note that equivalence between Newtonian and Brownian dynamics is not guaranteed when studying small length scales (as for example the decay of density fluctuations at large q), i.e. for intra cage motion, since there the microscopic dynamics may affect the shape of the decay of the correlation function. This is most relevant in gel systems for which the cage length can be significantly larger than the particle size.

III. RESULTS

In this section we examine the results of our simulation in terms of the thermodynamic and dynamic quantities mentioned above. We focus our attention on the cases $n_{\max} = 3$ and $n_{\max} = 4$, where a significant suppression of the liquid-gas spinodal as compared to the SW case is observed[33]. The suppression of the critical temperature and the shrinking of the unstable region in the $(\phi - T)$ plane makes it possible to study in one-phase conditions state points characterized by an extremely slow dynamics. More precisely, it is possible to study without encountering phase separation all $\phi \gtrsim 0.2$ for $n_{\max} = 3$ and $\phi \gtrsim 0.30$ for $n_{\max} = 4$. In the SW case, phase separation was encountered already at $T \approx 0.32$, when particle mobility is always large[49].

A. Phase Diagram

Ref. [33, 61] show that constraining the number of bonded neighbors reduces the energetic driving force for particle clustering. Therefore, as n_{\max} decreases, the phase separation transition (that we monitor by studying its spinodal), and the percolation line both shift to lower T (along isochores) and lower ϕ (along isotherms).

Fig. 1 reports the percolation and spinodal loci for $n_{\max} = 3$ (a) and $n_{\max} = 4$ (b). To evaluate the location of the spinodal line we interpolate the pressure $P(\phi)$ and search for the condition $dP/d\phi = 0$. To better track down the spinodal and estimate the effect of the spinodal in its vicinity we also determine the loci of constant $S(q \rightarrow 0)$, that we name ‘iso- $S(0)$ lines’, that can be considered as precursors of the spinodal line. Indeed, $S(0)$ is connected to the isothermal compressibility $\kappa_T = (d\phi/dP)/\phi$ by $S(0) = \rho k_B T \kappa_T$. The iso- $S(0)$ lines are calculated as loci of constant $(dP/d\phi)/k_B T$. We cross-check these estimates with the less precise value obtained calculating directly $S(q \rightarrow 0)$. The iso- $S(0)$ lines are shown to emphasize that, in bonded systems, an increase at small- q in the scattering intensity can arise in the one-phase region due to the vicinity of the spinodal curve.

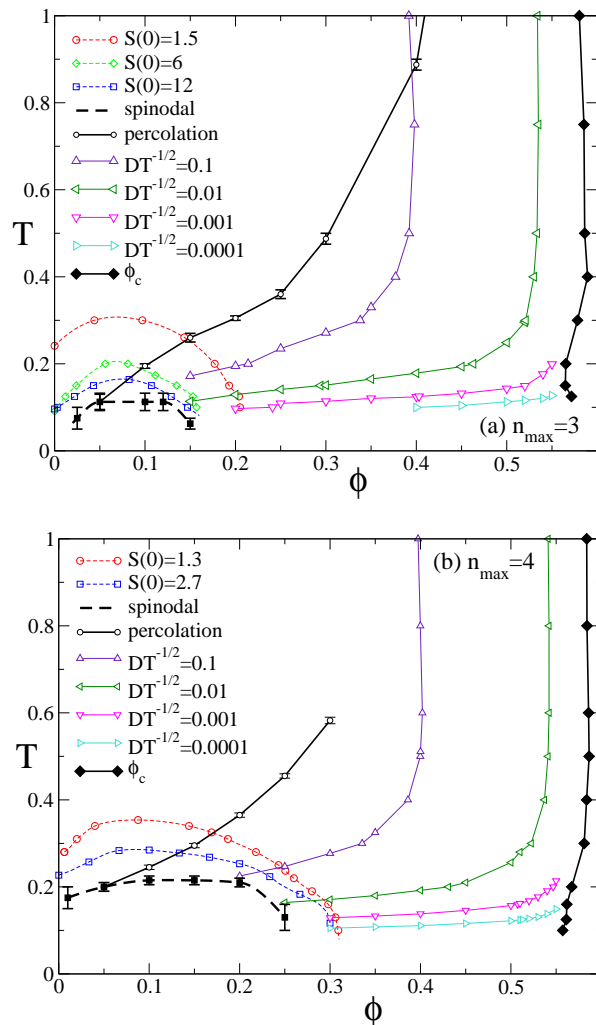


FIG. 1: Phase diagram for $n_{\max} = 3$ (a) and $n_{\max} = 4$ (b), showing the spinodal (dashed lines with squares), percolation (solid lines with open circles), iso-diffusivity loci where $D/\sqrt{T} = \text{constant}$ (lines with triangles), ‘iso- $S(0)$ lines’ (dashed lines). Also shown is the extrapolated *glass* line, labeled as ϕ_c from power-law fits, see text.

Fig. 1 also shows iso-diffusivity lines, i.e. lines where D/\sqrt{T} is constant. The scaling factor \sqrt{T} is used to take into account the trivial contribution of the thermal velocity with T . The investigated values of D/\sqrt{T} cover four orders of magnitude. Such iso-diffusivity lines are precursors of the dynamical arrest transition, corresponding to $D \rightarrow 0$. Previous works [21, 22, 84] have shown that these lines provide estimates of the shape and location of the arrest line. The isodiffusivity lines show an interesting behavior. They start from the high- ϕ side of the spinodal curve and then end up tracking the high- T hard-sphere limit. They are rather horizontal (parallel to the ϕ -axis) at low ϕ and rapidly cross to a vertical shape (parallel to the T -axis) at high ϕ . The crossing from horizontal to vertical becomes sharper and sharper on decreasing D/\sqrt{T} . In the SW case, the iso-diffusivity

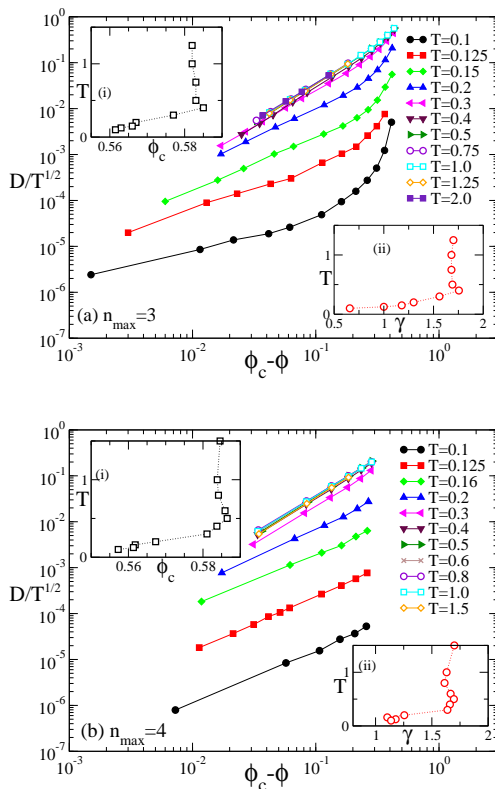


FIG. 2: Power law fit of inverse diffusivity $D^{-1} = A(\phi_c - \phi)^{-\gamma(T)}$ for (a) $n_{\max} = 3$ and (b) $n_{\max} = 4$. Lines are guides to the eye. Insets (a-i) and (a-ii) show the behavior of ϕ_c in the $\phi - T$ plane. Inset (b-i) and (b-ii) show the exponent γ as a function of T .

lines exhibit a reentrance in ϕ , in agreement with the predictions of the Mode Coupling Theory (MCT). The reentrance becomes more and more pronounced at lower and lower D/\sqrt{T} values. In the n_{\max} case, a reentrant shape is hardly observed. Indeed, in the SW the reentrance arises from the competition between cages created by the nearest neighbors excluded volume, with a typical hard-sphere localization length $\sim 0.1\sigma$, and cages created by bonding with a localization length $\sim \Delta$. In the n_{\max} case, such a competition becomes less effective due to the smaller number of bonds.

B. Estimation of dynamical arrest lines

To provide an estimate of the dynamical arrest lines, we can identify a range of parameters where the characteristic time follow a power-law dependence. In the case D is selected, data can be fitted according to $D^{-1}(\phi) = A(\phi_c - \phi)^{-\gamma(T)}$, where ϕ_c is the best estimate for the glass line. Fig.2 shows in log-log scale $D^{-1}(\phi)/\sqrt{T}$ vs $(\phi_c - \phi)$ for $n_{\max} = 3$ and $n_{\max} = 4$, where the ϕ_c values are chosen by a best-fit procedure. For $(\phi_c - \phi) \lesssim 0.3$, data are found to be well-represented by power-laws for at most two decades in D . The fits are performed over the range

$(\phi_c - \phi) < 0.3$. The T dependence of the fit parameters is also reported in Fig.2. The two fit parameters vary almost in phase with each other for both n_{\max} values. At high temperatures ($T \gtrsim 0.3$) attraction does not play a role, the arrest line is almost vertical and ϕ_c and γ are practically constant. For $T \lesssim 0.3$ smaller values of ϕ_c and γ are found. The values of γ are rather small at high T , close to the lowest possible value allowed by MCT, and become smaller than the lowest possible value allowed by MCT at low T . We note on passing that crystallization limits the ϕ range over which dynamic measurements in (metastable) ‘equilibrium’ can be performed. The region where we detect crystallization varies with T . At high T crystallization happens already for $\phi > 0.54$, while at low T , crystallization does not intervene up to $\phi = 0.56$. Thus, we cannot fully rely on the high T fits as $(\phi - \phi_c)$ is always large. Notwithstanding this, the estimate $\phi_c \approx 0.58$ is reasonable. On the other hand, at low T , the vicinity to ϕ_c increases, but the range of D values over which a power-law can be fitted decreases to about one decade, making the fit questionable. The fact that γ decreases well below the lowest meaningful MCT value could tentatively be associated to a difficulty of the theory to handle the crossing to an energetic caging (see also below). The resulting $\phi_c(T)$ line is also reported in Fig. 1. Independently of the fitting procedure, a clear vertically shaped arrest line, driven mostly by packing, is observed on isothermal compression.

To provide a better estimate of the arrest line at low ϕ we have studied the behavior of D with T along isochores. We have tried two routes. The first one consists in performing again power law fits but in temperature along an isochore, i.e. $D(T) \sim A(T - T_c)^{\gamma T}$, selecting an appropriate T -interval. For both $n_{\max} = 3$ and 4, such fits appear to hold for a rather small interval in D and are strongly dependent on the chosen T -interval selected in the fit procedure. In this way, we cannot extract a reliable estimate for T_c . Indeed, for the same state point T_c could vary from 0.2 to 0.08 depending on the fitting interval. However, fixing a T -interval of fitting for all isochores, the resulting $T_c(\phi)$ is again rather flat for both n_{\max} values. The second route is more robust and is based on the observed low T behavior, where data are found to follow very closely an Arrhenius law. Fig. 3 shows D as a function of $1/T$, for both $n_{\max} = 3$ and 4. Arrhenius behavior of D is observed at all ϕ at low T . The activation energy is around 0.45 for $n_{\max} = 3$ and of 0.55 for $n_{\max} = 4$. Since at the lowest studied temperatures the structure of the system is already essentially T -independent (see later on the discussion concerning Fig.5), there is no reason to expect a change in the functional law describing the $T \rightarrow 0$ dynamics. In this respect, the true arrest of the dynamics is located along the $T = 0$ line, limited at low ϕ by the spinodal and at high ϕ by crossing of the repulsive glass transition line. This peculiar behavior is possible only in the presence of limited valency, since when such a constraint is not present, phase separation preempts the possibility

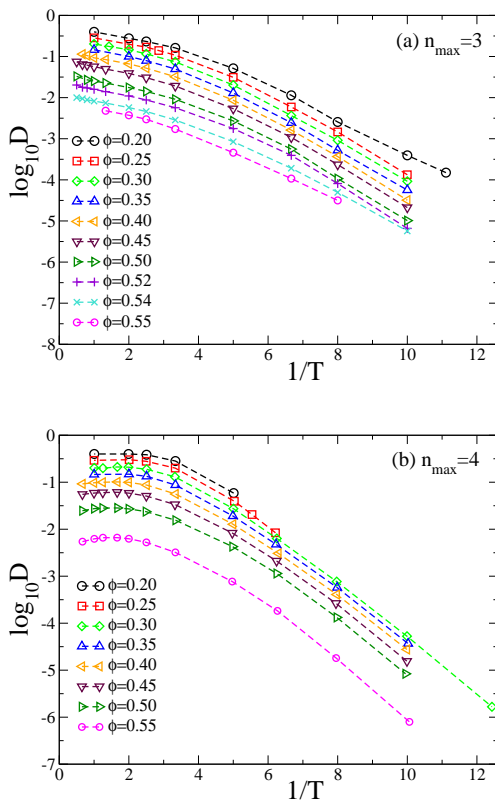


FIG. 3: Arrhenius plot of D for $n_{\max} = 3$ (a) and 4 (b) along all studied isochores without intervening phase separation.

of accessing the $T \rightarrow 0$ Arrhenius window.

We can summarize the dynamical arrest behavior in Fig. 4. One locus of arrest is found at high ϕ , rather vertical and corresponding to the hard-sphere glass transition. The isodiffusivity lines suggest a rather flat arrest line. Two different loci could be associated to arrest at low T . One defined by the T_c of the power-law fits and one at $T = 0$ associated to the vanishing of D according to the Arrhenius law. Notwithstanding the problem with the power-law fits and the big undeterminacy on T_c , it would be tempting to associate the T_c -line to the attractive glass line, at least as a continuation of it at low ϕ , and interpret the wide region between the two lines as a region of activated bond-breaking processes[80]. Data reported in the next sections will show that, in the present model, the identification of such line with an attractive glass line (or its extension to low density) is not valid, independently of the fit results. Indeed, we will show that particles are never localized within the attractive well width Δ , at any ϕ . On the other hand, the establishment of a percolating network of long-lived bonds, that we will refer to as a *gel* is identified. Ref. [33] shows that arrested states at low ϕ and T are profoundly different from both attractive and hard-sphere glasses. Now we are going to investigate if on increasing ϕ there is a crossover or a transition from gel to attractive glass, or whether the attractive glass exists at all in limited-valency models. We

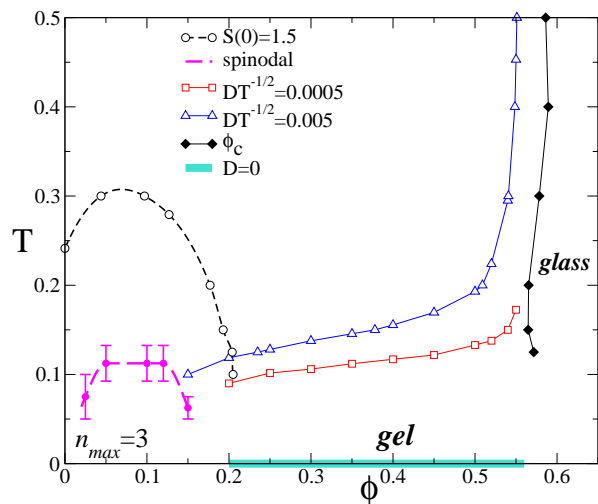


FIG. 4: Summary of the thermodynamic and kinetic phase diagram for $n_{\max} = 3$, including spinodal (dashed lines with filled circles), iso-diffusivity loci where $D/\sqrt{T} = 0.0005, 0.0005$ (lines with triangles and squares), iso- $S(0)$ locus where $S(0) = 1.5$, extrapolated *glass*, labeled as ϕ_c , and *gel*, labeled as $D = 0$, lines respectively from power law and Arrhenius fits ($T_c = 0$), see text.

refer the reader to a future work to compare these results with corresponding MCT predictions for the same model [85].

C. Static structure factor

This section reports results for the static structure factors for various studied T and ϕ and both $n_{\max} = 3$ and $n_{\max} = 4$. Results along an isochores and an isotherm are general for both studied n_{\max} values.

Fig. 5a shows the evolution with temperature of $S(q)$ at the lowest accessible ϕ (i.e. the lowest ϕ where phase separation is not present). On lowering T , $S(q)$ shows an increase of the intensity at small wave vectors, which saturates to a constant value when most of the bonds have been formed. This indicates that the system becomes more and more compressible, with large inhomogeneities, characterizing the *equilibrium* structure of the system. The inhomogeneities can be seen as an echo of the nearby phase separation or, equivalently, as a consequence of building up a fully connected network of particles with low coordination number. The large signal at small q is a feature of $S(q)$ which is often observed in gel samples [27, 86]. However, sometimes it may be difficult to discriminate between a true equilibrium gel and an arrested state generated through spinodal decomposition. In the present model, where phase separation is confined to the low ϕ region of the phase diagram, it is possible to reach in equilibrium extremely low T , making it possible to study reversible gel formation.

Besides the low- q growth, on cooling $S(q)$ shows a pro-

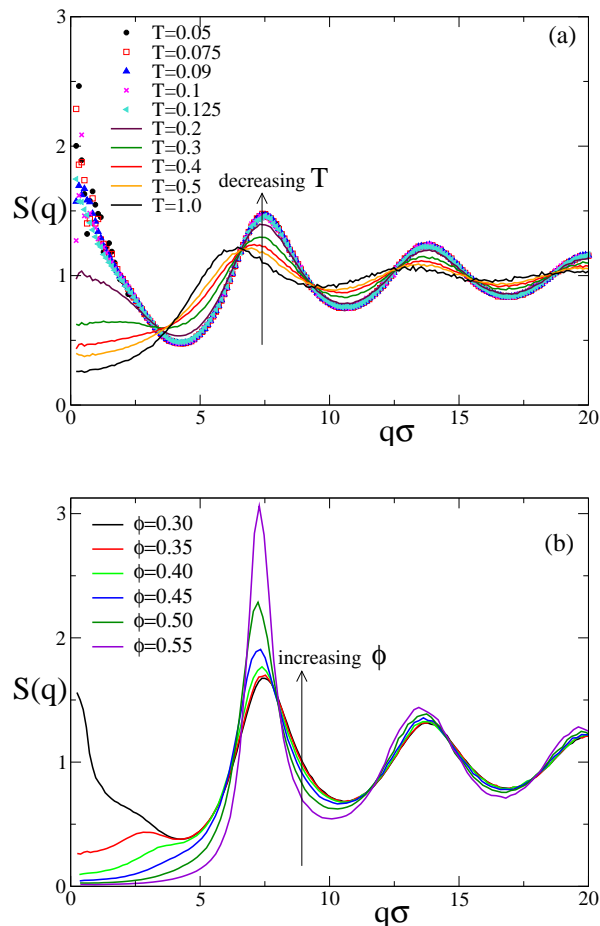


FIG. 5: (a) Evolution of the static structure factor $S(q)$ with T for the $\phi = 0.20$ isochores for $n_{\max} = 3$. Below $T = 0.125$ the system has reached an almost fully connected state and $S(q)$ does not change any longer with T ; (b) Evolution of the static structure factor $S(q)$ with ϕ for the $T = 0.125$ isotherm for $n_{\max} = 4$.

gressive structuring of peaks at $q\sigma \sim 2\pi$ and multiples thereof, signaling the fact that particles progressively become more and more correlated through bond formation. Indeed, the potential energy of the system progressively approaches the ground state value, where all particles have n_{\max} bonds [87]. Fig. 5b shows the evolution of $S(q)$ on increasing ϕ along a low T isotherm. Moving further from the spinodal, the $q \rightarrow 0$ peak decreases. A small pre-peak, around $q\sigma \approx 3$ is present at low densities, and persists with smaller intensity also at intermediate ϕ . Beyond $\phi \simeq 0.45$, a significant growth of the nearest-neighbour peak is found, signaling the increasing role of packing.

D. Mean squared displacement and caging

One of the hallmarks of glassy dynamics is the caging of a particle by its immediate neighbors. Caging is most easily seen in a log-log plot of the the mean squared

displacement (MSD) vs time as an intermediate-time plateau, separating short-time ballistic intracage motion and long-time diffusion out of the cage. The height of the plateau in the MSD provides a typical (squared) value for the localization length l_0 of the particles within the arrested state. For the standard HS glass, l_0 is found to be roughly 0.1σ , and corresponds to the average distance a particle can explore rattling within its nearest neighbour cage. For an attractive glass, on the other hand, l_0 corresponds to the attractive well-width, since particles are forced to rattle within the bond distance. For this reason, the MSD plateau is significantly smaller than for the HS glass (of the order $\Delta^2 \approx 10^{-3}$ versus $(0.1\sigma)^2 \approx 10^{-2}$). For the same reason, the q -width of f_q is significantly larger for the attractive glass solution than for the repulsive one.

In the low- ϕ study reported in [33], on isochoric cooling a clear plateau develops in the MSD, but its value indicates a very high localization length, of the order of one or more particle diameters. The localization length does not change appreciably with T , even below T_c . We attributed this finding to the presence of a long-living percolating network of particles allowing for ample single particle movements (arising from the gel "vibrational" modes) which completely mask the bond localization. In this respect, the connectivity of the network plays an important role in the slowing down and provides an additional mechanism of arrest with respect to both attractive and repulsive glasses.

Here we study the high- ϕ behavior with the aim of locating the cross-over from low- ϕ arrest (gel) to the high- ϕ case and to see if a crossover or transition emerges to one of the above cited glasses. Results for the ϕ dependence of the MSD along a low T isotherm are presented in Fig. 6 for $n_{\max} = 3$ and 4. Both graphs show similar features. A very high plateau of order unity, slightly decreasing with ϕ , is found up to $\phi \approx 0.45$. Although the long-time dynamics is monotonically slower with increasing ϕ , the plateau becomes less defined near $\phi = 0.50$, slowly crossing over to a quite distinct plateau compatible with the HS one at $\phi = 0.55$ for $n_{\max} = 4$ and at $\phi = 0.56$ for $n_{\max} = 3$.

Defining the cage length l_0 as the square root of the MSD value at the inflection point of the MSD in log-log scale we plot l_0 in the insets of Fig. 6. The cage length starts from values larger ($n_{\max} = 3$) or close ($n_{\max} = 4$) to σ and progressively approach the HS limiting value 0.1σ .

In a window of ϕ values, the crossover between the two plateaux in the MSD displays a sub-diffusive behavior for up to two decades in time, i.e. $\langle r^2 \rangle \propto t^\alpha$, with a state-point dependent exponent $\alpha < 1$. A similar behavior was found in the simulations of the SW system [22, 81], in a limited T -window, within the liquid reentrant region. In the SW case the subdiffusive behavior is found for MSD values between Δ^2 (the bond cage) and $10^{-2}\sigma^2$ (the HS cage) and it is due to a competition between attractive and HS glasses at low and high T . Ex-

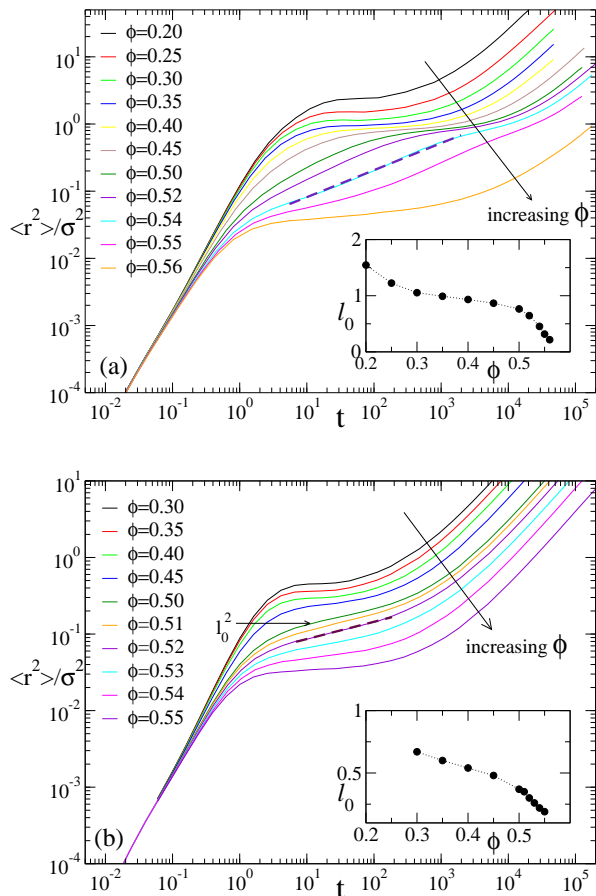


FIG. 6: Mean squared displacement (MSD) and caging. (a) MSD along $T = 0.1$ for $n_{\max} = 3$; (b) MSD along $T = 0.125$ for $n_{\max} = 4$. The insets show the localization length l_0 as a function of ϕ , with dotted line as guide to the eye. Dashed lines highlight subdiffusive behavior at intermediate ϕ .

PLICIT MCT predictions have confirmed this feature[88], connecting it with the presence of a near-by higher order singularity. In the present case it appears that the subdiffusive behavior arises from the competition between the very different localization lengths of the gel-arrested network and the HS glass. The MSD phenomenology is reminiscent of that found in presence of a higher order MCT singularity[89]. It is possible that the subdiffusive behavior (and other features such as the logarithmic decay of the density auto-correlation functions discussed later on) arise generically from the competition between two disordered arrested states.

E. Density Relaxation, Bond Relaxation and Non-ergodicity

We now focus on the behavior of the density autocorrelation functions $F_q(t)$. Ref. [33] called attention on the different time dependence of the low and high q window. At small q , dynamics slow down significantly and become

non-ergodic, while at larger q (already on the scale of nearest neighbours) dynamics remain ergodic to within numerical accuracy. At low density, the non-ergodicity parameter for the gel is different from that of either the repulsive or attractive glass. We now investigate the effect of density on these findings.

To provide a picture of the behavior of the dynamics at low T as a function of ϕ we plot in Fig. 7 the density correlators for three different values of q , corresponding to distances respectively much larger, larger, and comparable to the nearest neighbor distance σ . In addition, we report the behaviour of the bond correlation function $\phi_B(t)$ at the same low T , for small and large ϕ .

The ϕ -evolution of the shape of the correlation function is particularly complex. At very small q , ($q\sigma \sim 1$), all correlation functions show a clear plateau, followed by the α -relaxation process. Interestingly, the plateau value has a non-monotonic behavior with ϕ . It starts from an high value at the lowest ϕ and decreases down to less than 0.1 before increasing again on approaching the hard-sphere glass. At the present time, we have no explanation for these trends.

Even more complicated is the $q\sigma \sim 3$ case. The plateau value first increases with ϕ , then a reversal of the trend is observed at $\phi = 0.40$ where the plateau height starts to decrease. Such a decrease persists up to $\phi = 0.50$, after which a distinguishable plateau almost disappears. Correlators are higher at comparable times and become almost logarithmic for up to three time decades. At $\phi = 0.56$, a clear repulsive glassy behavior is recovered.

Much simpler is the interpretation of the last case, $q\sigma \sim 7$ (and larger q). Here, the standard scenario for the repulsive glass is observed, despite the presence of a connected long-living network of bonds. The absence of any detectable (within our numerical precision) plateau at small length scales and low ϕ confirms the ability of the particles to explore distances smaller than σ without any constraint. This is an effect of the loose character of the network, of the small overall ϕ (as compared to the typical HS glass values) and of the small local degree of connectivity.

Focusing on the behaviour of $\phi_B(t)$, we find that the curves follow closely, at all studied ϕ , a simple exponential law, i.e. a stretched exponential fit gives an exponent β always close to 1 (tending to 1 with decreasing T). From the figures, it is evident that bond relaxation is always much slower as compared to density relaxation even for very small q . This suggests that, up to at least a time of order 10, the density relaxation is coupled to the movements of a permanent network which, without breaking most of its bonds, is capable of spanning a large part of the simulation box. At longer times, the breaking of the bonds enters into play, producing a secondary very slow relaxation in $F_q(t)$, accompanied by very small plateau, as it is evident in panels (a) and (b) for small q .

On increasing n_{\max} , the same features for $F_q(t)$ are observed at a progressively larger q . An example is reported in Fig.8 for the case $q\sigma \sim 8$. Here, around $\phi = 0.52$ a log-

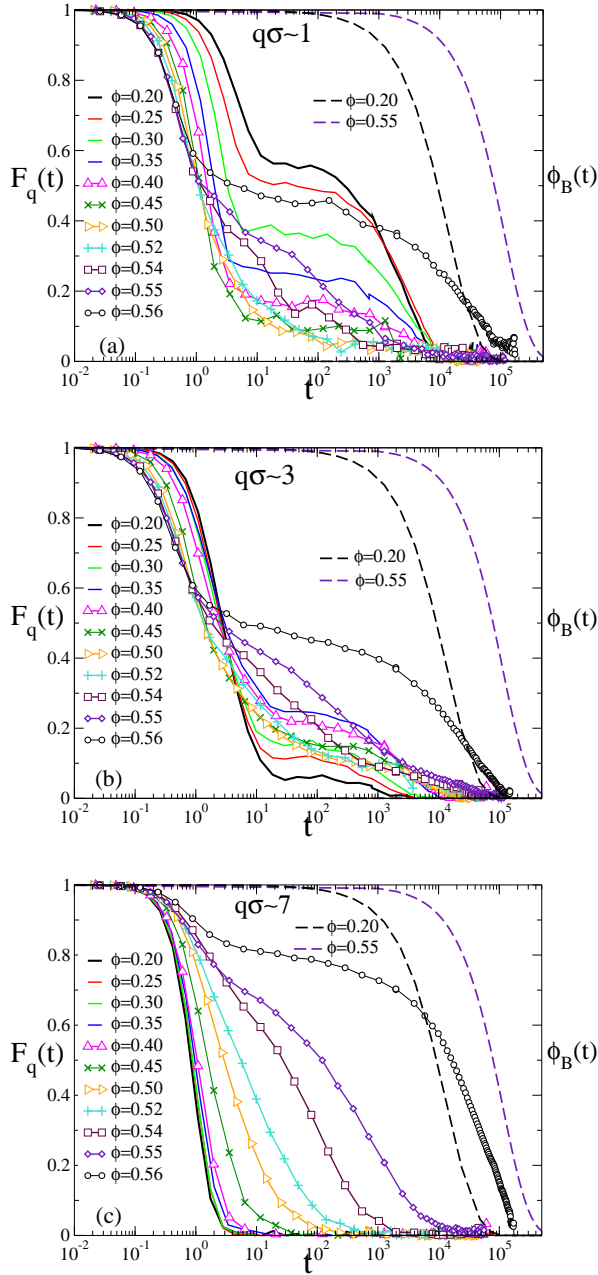


FIG. 7: Density autocorrelation functions for $T = 0.1$ and $n_{\max} = 3$ at various ϕ and $q\sigma \sim 1, 3, 7$. Also, bond correlation functions $\phi_B(t)$ (dashes lines) at small and large ϕ are reported in all three panels for comparison.

arithmetic decay for about two time decades is observed. At this wave-vector, corresponding to lengths smaller than the nearest neighbour one, the non-monotonic behavior of the plateau is not present anymore.

To better grasp the logarithmic behavior observed in Figures. 7 and 8, in Fig. 9 we show the q -dependence of $F_q(t)$ at $\phi = 0.54$, i.e. the ϕ showing the most enhanced $\log(t)$ dependence, for $n_{\max} = 3$. We note that the best (long-lasting) $\log(t)$ dependence is seen in a finite window of q -values, roughly between $3 \leq q\sigma \leq 6$,

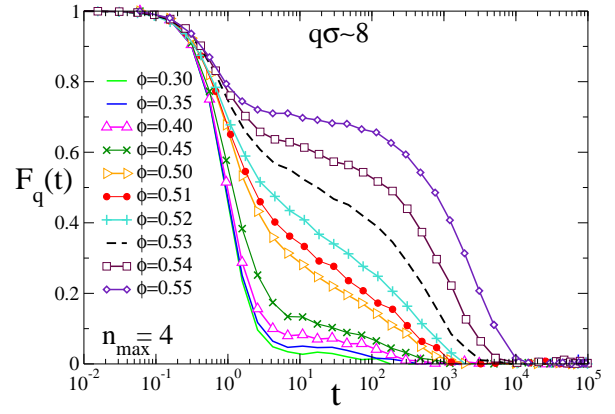


FIG. 8: Density autocorrelation functions for $T = 0.125$ and n_{\max}

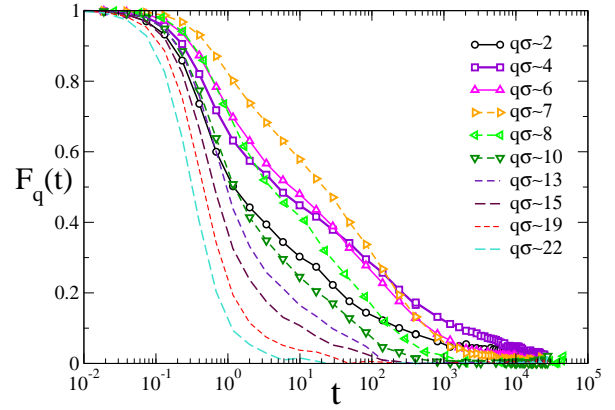


FIG. 9: Density autocorrelation functions for $T = 0.1$, $\phi = 0.54$ and $n_{\max} = 3$ at various $q\sigma$. A $\log(t)$ behavior is observed for $3 \leq q\sigma \leq 6$ for up to three time decades.

and it covers about three orders of magnitude in time. Again, on increasing n_{\max} this q -window shifts to larger q (approximately between $8 \leq q\sigma \leq 10$).

A possible quantification of the characteristic time of the dynamics and of the non-ergodicity parameter is provided by stretched exponential fits ($F_q(t) = f_q \exp(-(t/\tau_q)^{\beta_q})$) of the long time decay. This fit allows us to extract information on the behavior of the non-ergodicity parameter f_q , as well as on the stretching exponent β_q and an estimation of the relaxation time τ_q . Still, in a certain region of ϕ and q values, the decay of the correlators is clearly different from a stretched exponential, being $F_q(t)$ essentially linear in $\log(t)$. Under these conditions we cannot fit the density correlators and estimate the non-ergodicity parameter.

Fig. 10 shows f_q along the low T isotherm for $n_{\max} = 3$ and 4 for several ϕ . In both cases, a different non-ergodic behavior at low and high ϕ is evident. At low ϕ , f_q is largest at $q \rightarrow 0$, then decays rapidly to zero within a range of about 5 in units of $q\sigma$. With increasing ϕ , the overall height of f_q decreases, but a small peak starts to form at larger q , which is still of the order of a few $q\sigma$.

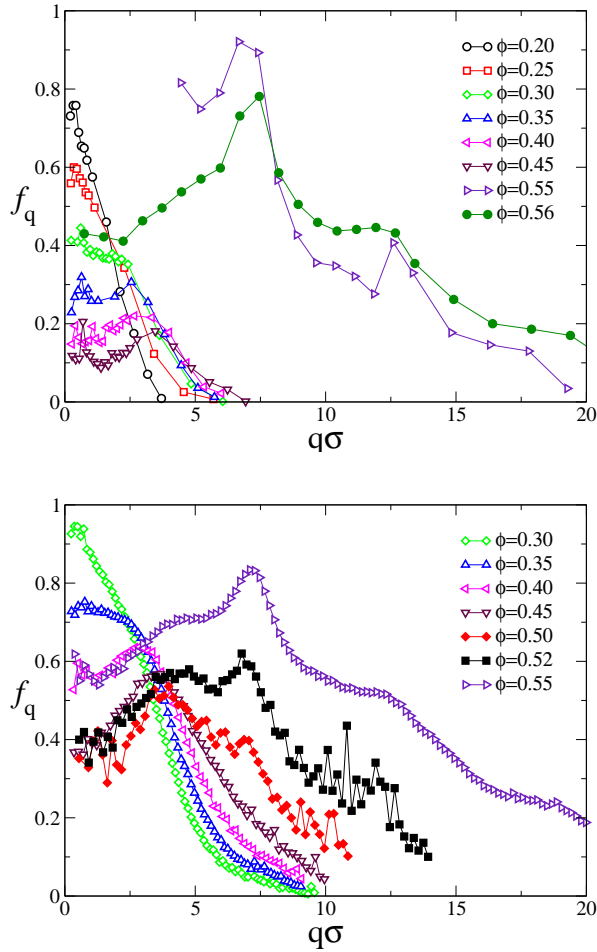


FIG. 10: Non-ergodicity factor, obtained from stretched exponential fits, at various ϕ for $T = 0.1$ and $n_{\max} = 3$ (a) and $T = 0.125$ and $n_{\max} = 4$ (b).

This behavior roughly follows that of $S(q)$, for which the low q increase turns to a small peak at finite q (see for example in Fig.5b). At large ϕ the shape of f_q closely resembles that of a hard sphere system, with the first peak around $q\sigma \approx 2\pi$, i.e. the nearest neighbour length scale.

At intermediate ϕ , we observe a slightly different behavior between the two studied values of n_{\max} . As discussed before, for $n_{\max} = 3$ and $0.45 < \phi < 0.55$, we cannot estimate f_q from the fits. The reason for this is that $F_q(t)$ displays unusual features, like a logarithmic decay at certain q followed by a secondary relaxation reminiscent of the gel type. Fig. 10 shows that a sharp transition in the q dependence of f_q takes place between $0.45 < \phi < 0.55$, which we associate to the gel-to-glass transition. For $n_{\max} = 4$ there seems to be a smoother transition although a similar non-monotonic behavior of f_q with ϕ at low q is observed.

We further note that the relaxation time τ_q , extracted from the fits or otherwise, monotonically increases with ϕ despite the non-monotonicity in the plateau. The be-

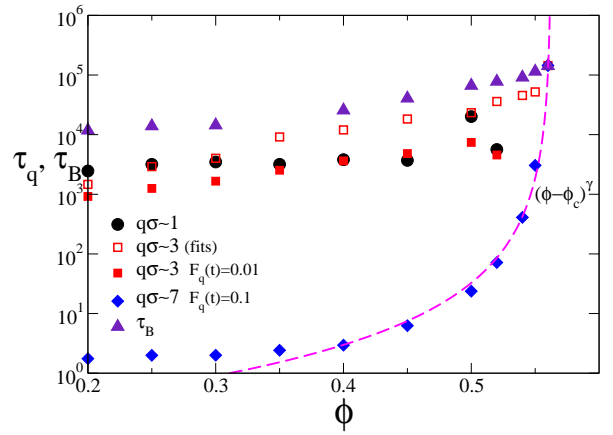


FIG. 11: ϕ -dependence of the density relaxation time τ_q at $q\sigma \sim 1, 3, 7$ versus bond relaxation time τ_B (triangles), at fixed $T = 0.1$ for $n_{\max}=3$. τ_q are either extracted from stretched exponential fits or via the relation $F_q(\tau_q) = 0.01$ ($q\sigma \sim 3$) and $F_q(\tau_q) = 0.1$ ($q\sigma \sim 7$). In the latter case, the dashed line is a fit of the data to a power law $(\phi - \phi_c)^\gamma$.

havior of τ_q with ϕ at low T is shown in Fig.11 at the q -values discussed above for $n_{\max} = 3$, together with the corresponding behavior for the bond relaxation time τ_B . Apart from the fits, τ_q can be also conventionally defined as the time at which the normalized correlators are equal to an arbitrary (low) value, which is chosen for convenience as 0.1. Doing so, for $q\sigma \sim 7$, we find that τ_q follows a typical, for glass-forming systems, power-law dependence on ϕ , also shown in the figure, with critical ϕ_c 0.562 and exponent $\gamma \approx 2.5$. This result for ϕ_c is quite consistent with that extracted from the diffusivity fits discussed earlier. However, on lowering q , the situation becomes more complicated. At $q\sigma \sim 3$, the conventional arbitrary value 0.1 is too high, since the correlators displays smaller plateau values. Thus, in Fig. 11 we report τ_q obtained both from the fits and by choosing a conventional value 0.01. The results are parallel to each other, and do not show a power law behavior. Rather there seems to be a crossover regime at intermediate ϕ . However, the relaxation time is monotonically increasing at this length scale of observation, despite the non-monotonic behavior of the plateau. At even lower q , e.g. $q\sigma \sim 1$, we cannot define a satisfying finite value for $F_q(t)$, below the plateaux at all studied ϕ and numerically detectable. Also the fits cannot be relied on at high densities. As shown in the inset, it seems that τ_q does not vary strongly with ϕ , and indeed all correlators (see Fig. 7a) seem to meet at $F_q(t) = 0$ at around the same value of t , up to $\phi = 0.52$.

A sensible estimate of τ_B is simply obtained by stretched exponential fits of $\phi_B(t)$. τ_B is always longer than the density relaxation time at all q , as remarked above. Moreover, the increase of τ_B upon ϕ , is rather small, indicating that bonds are slightly stabilized by crowding. τ_B is completely decoupled from τ_q at large q , while it becomes coupled to τ_q at small q , the data be-

ing almost parallel, and, it seems that in the limit $q \rightarrow 0$, the two relaxation times would coincide. Once again, we associate the large τ_B to the very slow secondary relaxation observed for density correlators at small q (see for example $q\sigma \sim 3$ and $0.50 \leq \phi \leq 0.55$ in Fig. 7b).

A final observation concerns the behavior of β_q extracted from the fits, outside the logarithmic regimes. We find at high q ($q\sigma \geq 7$) and low ϕ , that values of β_q are larger than 1, actually close to 1.5, associated more to a compressed than a stretched exponential [28, 90, 91]. However, this value decreases below 1 for high ϕ and large q , while it tends to be 1 for low ϕ and low q ($q\sigma \lesssim 7$). We note that care has to be taken when exponents greater than 1 are found in Newtonian dynamics, since they could arise from undamped motion of clusters (possibly of rotational origin), or elastic motion within the percolating structure. A comparison with a Brownian dynamics simulation may help to clarify this issue.

Additionally, we focus on the T dependence of the density correlators. In Ref.[33], we discussed the T dependence along the lowest isochore $\phi = 0.20$. There, we found that, only at low enough q , there was the emergence of a gel plateau at low T and that, in this region of wavevectors, the density relaxation time τ_q as well as the bond relaxation time τ_B both followed an Arrhenius law. On increasing density, there is the gel to glass crossover, which is clearly visible by looking at the T behavior of $F_q(t)$, as shown in Fig. 12. Up to $\phi = 0.45$ a clear gel plateau is approached. Beyond this value, the anomalously slow logarithmic decay is observed, at its best for $\phi = 0.54$, reported in figure 12(a). Above this ϕ , e.g. $\phi = 0.55$ in 12(b), a crossover from logarithmic to standard glass regime (i.e., typical two-step relaxation) is observed. A clear difference between these two graphs is the fact that at $\phi = 0.54$ pure logarithmic decay is observed up to the lowest T , while at $\phi = 0.55$ a kink, evidence of the nearby glass transition, is present. We also note that, interestingly, the shape of the correlators in Fig. 12(b) is very reminiscent of Fig.11 in Ref.[13] and Fig.6 in Ref.[22], respectively MCT predictions and simulation results for the SW model, for fixed temperature in the reentrant region and varying density. Here, the analogous plot is reported, at a density within the gel to glass crossover, and varying T . Again, this suggests a close similarity of the features at the gel to glass crossover with respect to the SW crossover from repulsive to attractive glass.

Finally, both the relaxation time τ_q and the bond relaxation time τ_B are found to obey Arrhenius dynamics in T at all ϕ .

IV. DISCUSSION

The interpretation of these results is not completely straightforward. However, they strongly suggest that the system gels at low ϕ and forms a glass at high ones. It is important to understand what happens in between these

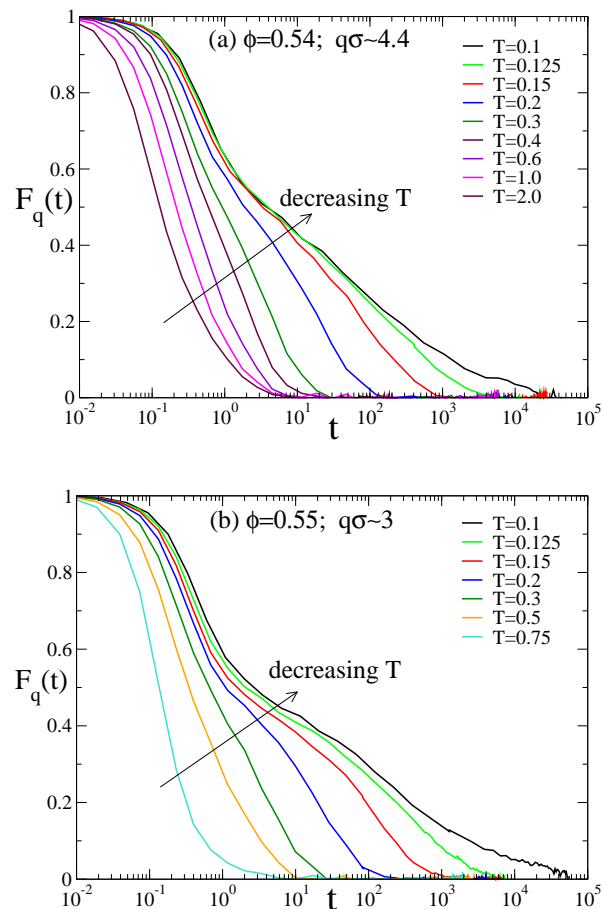


FIG. 12: Density autocorrelation functions for $n_{\max} = 3$ at various studied T for (a) $\phi = 0.54$ and $q\sigma \sim 4.4$ (maximally enhanced $\log(t)$ behavior) and (b) $\phi = 0.55$ and $q\sigma \sim 3$ (interference between $\log(t)$ behavior and standard glass-like α -relaxation).

two regimes, where a new type of relaxation takes place, as a result of the competition of the two effects. Similarly to the simple SW case, where anomalous dynamics arises in the reentrant liquid region from the competition between attractive and repulsive glass, here again anomalous dynamics is generated from the presence of two distinct arrested states. However, in the attractive-vs-repulsive glass scenario, temperature is the control parameter generating a liquid pocket in between. Here ϕ is the control parameter. We have to bear in mind that at $T = 0.1$ the energy per particle of the system for $n_{\max} = 3$ varies from about -1.48 at $\phi = 0.20$ to about -1.495 at $\phi = 0.56$, indicating that most of the particles ($\approx 99\%$) are fully bonded (i.e. they have reached the n_{\max} limit already). With increasing ϕ , more neighbors surround each particle but only n_{\max} of them interact via an attractive well, the others probing only the hard core interaction. Thus we cannot expect a non-monotonic ϕ dependence of the characteristic time (i.e. no re-entrance).

Where does the logarithm/subdiffusivity come from? A more intuitive understanding of the anomalous dynamics results from interpreting the MSD behavior. If one thinks simply of a filling up of space, the MSD plateau should monotonically decrease and no subdiffusive behavior should be observed. However, at $\phi \approx 0.54$ a clear t^α law is observed. After the ballistic regime, particles start to feel the presence of the nearest-neighbours and the MSD slows down. At long times, particles are able to break and reform the bonds, the network fully restructures itself and proper diffusion is observed. In the intermediate time window one observes the competition between excluded-volume confinement and exploration of space associated to the motion of the unbroken network. We believe that this is at the origin of the anomalously slow diffusion and logarithmic decay.

To support this hypothesis we note that the logarithmic decay shows up only in a window of small q 's significantly less than the nearest-neighbour inverse length (i.e. over distances where connectivity is probed). On increasing n_{\max} , this length becomes smaller due to the higher degree of constraint for the network, in the same way as the localization length, estimated from the MSD, decreases. However, we recall that in the SW system such anomalous $\log(t)$ decay was observed for very large q , associated to the typical distance of the short-range attraction. This provides further evidence that in the n_{\max} case the connectivity of the network is associated with generating unusual $\log(t)$ features and confirming that the width of the attractive well does not play any significant role.

A final comment regards the existence of the so-called higher order MCT singularity. In the SW case, the width of the attraction Δ is the crucial control parameter driving the system close to the singularity. In the n_{\max} case, Δ does not play a relevant role. It is intriguing to ask ourselves which parameter plays the role of Δ , if the gel-to-glass cross over belongs to the same class of models possessing a higher order MCT singularity. One possible answer is n_{\max} itself. Indeed, we noted how the characteristic length scale to observe logarithmic behavior in $F_q(t)$ shifts with increasing n_{\max} . Our present knowledge is that this is found at $q\sigma \approx 4$ for $n_{\max} = 3$ and $q\sigma \approx 8$ for $n_{\max} = 4$. We also know that for the SW, although being associated to the competition of repulsive and attractive glasses, it moves up to $q\sigma \sim 20$ [81]. The possible existence of a smooth crossover between the two phenomena could be theoretically investigated with simulations. However, the existence of the higher order singularity in the present model is destined to be uncertain, unless some theory is devised for the gel transition and its predictions tested against the simulations.

V. CONCLUSIONS

Understanding the slowing down of the dynamics in colloidal systems and the loci of dynamic arrest in the

full $(\phi - T)$ plane, encompassing gel and glass transitions, is one of the open issues in soft condensed matter. Two classes of potentials have been explored in some details in the recent years: (i) short-range attractive spherical potentials and (ii) short-range attractive spherical potentials complemented with a repulsive shoulder. In the first case, it has been shown that low ϕ arrested states arise only as a result of a interrupted phase separation. The second case appears to be much more complicated and partially unresolved. For certain values of the parameters of the repulsive potential the system separates into clusters (which can be interpreted as a mesoscopic interrupted phase separation) and dynamic arrest at low ϕ can follow from a cluster glass transition or from cluster percolation.

In the attempt to provide an accurate picture of dynamics and a model for dynamic arrest at low ϕ in the absence of phase separation (both at the macroscopic and mesoscopic level) we present here a study of a minimal model of gel-forming systems. The model builds up on the intuition that phase separation is suppressed when the number of interacting neighbors becomes less than six, since the energetic driving force for phase separation becomes less effective[92]. To retain the spherical aspect of the potential, a standard SW interaction potential is complemented by a constraint on the maximum number n_{\max} of bonded neighbors (a model similar to the one first introduced by Speedy and Debenedetti[64, 65]).

In this manuscript we have presented a detailed study in the (ϕ, T) plane of the dynamics for $n_{\max} = 3$ and $n_{\max} = 4$. For these two values of n_{\max} the region of phase diagram where unstable states (with respect to phase separation) are present shrinks to $T \lesssim 0.1$ and $\phi \lesssim 0.3$, making it possible to approach on cooling low ϕ arrested states, technically in metastable (with respect to crystallization) equilibrium. The simplicity of the model makes it possible to study it numerically even at very low T and estimate, with accuracy, the low- T fate of the supercooled liquid. It becomes possible to predict the regions in the phase diagram where disordered arrested states are kinetically stabilized as compared to the lowest free energy crystalline states.

Dynamics in the n_{\max} model is also important because it provides a zero-th order reference system for the dynamics of particles interacting via directional potentials. These systems include globular protein solutions (hydrophilic/hydrophobic patches on the surfaces of proteins), the new generation of patchy colloids, and, at a smaller scale, network forming liquids. In this respect, the n_{\max} model allows us to study the generic features (since it neglects the geometric correlations induced by directional forces) of particle association. It has the potential to provide us with an important reference frame to understand dynamical arrest in network-forming liquids and the dependence of the general dynamic and thermodynamic features on the number of patchy interactions.

One of the important results is contained in Fig. 1, which shows the locus of iso-diffusivity in the $(\phi - T)$

plane. These lines, which provide an accurate estimate of the glass transition line ($D \rightarrow 0$) are found to be essentially vertical at high ϕ , in correspondence to the HS glass transition, and essentially horizontal at low T . Only a very weak, almost negligible, reentrance in ϕ is observed. Extrapolating the D -dependence by power laws in ϕ and by Arrhenius laws in T , we estimate the glass-lines. The Arrhenius law is found to be valid for many decades, suggesting that, at intermediate ϕ , D vanishes only at $T = 0$. Data strongly support the possibility of two distinct arrest transitions: a glass of the HS type driven only by packing at high ϕ and a gel at low T [93].

We have chosen the word *gel* to label arrest at small and intermediate ϕ since the analysis of the simulation data confirms that the establishment of a network of bonded particles and the network connectivity plays a significant role in the arrest process. While particles are locally caged by SW bonds with n_{\max} neighbors (and in this respect one would be tempted to name it an attractive glass), particle localization is not only controlled by bonding. Bonded particles are free to explore space (retaining their connectivity) until they are limited by the network constraints. Indeed, the plateau of the MSD is, especially at the lowest ϕ , larger than the particle size. We remark that the bond localization, typical of the attractive glass case, is not observed throughout the phase diagram, neither in the MSD nor in the width of f_q . We believe this is due to the fact that, although bonding is present, particles are confined by the potential well only relative to each other. The network connectivity length is the quantity that enters into the determination of the localization length in the arrested state. On increasing ϕ , the localization length progressively approaches the one characteristic of the hard-sphere glass, signaling that a cross-over to the excluded volume case takes place.

The intersection between the repulsive glass and gel loci appears to be associated to anomalous dynamics. No intermediate liquid state, i.e. no reentrant regime in ϕ , is found. Interestingly enough, these anomalies are strongly reminiscent of the anomalies observed close to the intersection of the attractive and repulsive glasses in the case of short-range interacting particles. Correlation functions show a clear $\log(t)$ dependence in a window of q vectors and the MSD shows a clear subdiffusive behavior $\sim t^\alpha$. Here, the gel localization length is larger than of the HS glass, a different scenario from the attractive-

repulsive case. These results support the hypothesis that a possible MCT-type higher order singularity in the n_{\max} model is present and, at the same time, provide further support to the intrinsic difference in the localization mechanisms that are active for the two arrested states. In contrast to the SW case, the well-width is not a crucial length scale in the problem, while an important parameter is n_{\max} , that could be the control parameter of a putative higher order singularity of the MCT type.

One further consideration refers to the role of Δ in the n_{\max} model. We have chosen to use $\epsilon \equiv \Delta/(\sigma + \Delta) = 0.03$ to connect with the well studied corresponding SW case. We do not expect significant differences for the two arrested states for Δ values up to $\epsilon \approx 0.1 - 0.2$, since the connectivity properties would be essentially identical. Thus, we still expect the existence of distinct gel and glass lines. Only the interplay between the two could be affected, as for example the $\log(t)$ behavior should be shifted in its q -dependence. Also, in that case, the behavior with n_{\max} is not a priori clear, since for larger Δ values no MCT singularity is present for the SW model and, from a theoretical point of view, the attractive glass line is not physically distinct from the repulsive one.

In summary, the present model provides a clear indication that even if liquid-gas phase separation can be avoided and arrest at low ϕ can be explored in equilibrium conditions, the observed arrested state is not the low- ϕ extension of the attractive glass. The present results strongly suggest that the attractive glass is an arrested state of matter which can be observed in short-range attractive potentials only at relatively high ϕ , being limited by the spinodal curve. When the interparticle potential favors a limited valency, arrest at low ϕ becomes possible but with a mechanism based on the connectivity properties of a stable particle network, clearly different from what would be the extension of the (attractive) glass line.

VI. ACKNOWLEDGMENTS

We acknowledge support from MIUR-Cofin, MIUR-Firb and MRTN-CT-2003-504712. I. S.-V. acknowledges NSERC (Canada) for funding. We thank T. Voigtmann and W. Kob for useful discussions.

-
- [1] A. Yethiraj and A. V. Blaaderen, *Nature* **421**, 513 (2003).
 - [2] W. B. Russel, D. A. Saville, and W. R. Schowaltes, *Colloidal Dispersions*, Cambridge University Press, Cambridge, 1991.
 - [3] J.-L. Barrat and J.-P. Hansen, *Basic Concepts for Simple and Complex Liquids*, Cambridge University Press, Cambridge, 2003.
 - [4] D. Frenkel, *Science* **296**, 65 (2002).
 - [5] F. Sciortino and P. Tartaglia, *Advances in Physics* **54**, 471 (2005).
 - [6] W. van Meegen and S. M. Underwood, *Phys. Rev. Lett.* **70**, 2766 (1993).
 - [7] G. Bryant et al., *Phys. Rev. E* **66**, 060501 (2002).
 - [8] P. N. Pusey and W. van Meegen, *Phys. Rev. Lett.* **59**, 2083 (1987).
 - [9] S. Asakura and F. Oosawa, *J. Polym. Science* **33**, 183 (1958).

- [10] C. N. Likos, Phys. Rep. **348**, 267 (2001).
- [11] L. Fabbian, W. Götze, F. Sciortino, P. Tartaglia, and F. Thiery, Phys. Rev. E **59**, 1347 (1999).
- [12] J. Bergenholtz and M. Fuchs, Phys. Rev. E **59**, 5706 (1999).
- [13] K. A. Dawson et al., Phys. Rev. E **63**, 011401 (2001).
- [14] F. Mallamace et al., Phys. Rev. Lett. **84**, 5431 (2000).
- [15] K. N. Pham et al., Science **296**, 104 (2002).
- [16] T. Eckert and E. Bartsch, Phys. Rev. Lett. **89**, 125701 (2002).
- [17] S. H. Chen, W.-R. Chen, and F. Mallamace, Science **300**, 619 (2003).
- [18] D. Pontoni, T. Narayanan, J.-M. Petit, G. Grübel, and D. Beysens, Phys. Rev. Lett. **90**, 188301 (2003).
- [19] J. Grandjean and A. Mourchid, Europhysics Letters **65**, 712 (2004).
- [20] A. M. Puertas, M. Fuchs, and M. E. Cates, Phys. Rev. Lett. **88**, 098301 (2002).
- [21] G. Foffi et al., Phys. Rev. E **65**, 050802 (2002).
- [22] E. Zaccarelli et al., Phys. Rev. E **66**, 041402 (2002).
- [23] E. Zaccarelli et al., Phys. Rev. Lett. **92**, 225703 (2004).
- [24] A. M. Puertas, E. Zaccarelli, and F. Sciortino, J. Phys.: Condens. Matter **17**, L271 (2005).
- [25] N. A. M. Verhaegh, D. Asnaghi, H. N. W. Lekkerkerker, M. Giglio, and L. Cipelletti, Physica A **242**, 104 (1997).
- [26] P. N. Segrè, V. Prasad, A. B. Schofield, and D. A. Weitz, Phys. Rev. Lett. **86**, 6042 (2001).
- [27] S. A. Shah, Y. L. Chen, S. Ramakrishnan, K. S. Schweizer, and C. F. Zukoski, J. Phys.: Condens. Matter **15**, 4751 (2003).
- [28] L. Cipelletti and L. Ramos, J. Phys.: Condens. Matter **17**, 253 (2005).
- [29] S. K. Kumar and J. F. Douglas, Phys. Rev. Lett. **87**, 188301 (2001).
- [30] F. Sciortino, S. Mossa, E. Zaccarelli, and P. Tartaglia, Phys. Rev. Lett. **93**, 055701 (2004).
- [31] A. Coniglio, L. De Arcangelis, E. Del Gado, A. Fierro, and N. Sator, J. Phys.: Condens. Matter **16**, S4831 (2004).
- [32] F. Sciortino, P. Tartaglia, and E. Zaccarelli, J. Phys. Chem. B **109**, 21942 (2005).
- [33] E. Zaccarelli et al., Phys. Rev. Lett. **94**, 218301 (2005).
- [34] E. Del Gado and W. Kob, (2005), preprint cond-mat/0507085.
- [35] J. Bergenholtz, W. C. K. Poon, and M. Fuchs, Langmuir **19**, 4493 (2003).
- [36] K. Kroy, M. E. Cates, and W. C. K. Poon, Phys. Rev. Lett. **92**, 148302 (2004).
- [37] A. Puertas, M. Fuchs, and M. E. Cates, Phys. Rev. E **67**, 031406 (2003).
- [38] P. J. Flory, J. Am. Chem. Soc. **63**, 3083 (1941).
- [39] M. Rubinstein and A. V. Dobrynin, Curr. Opin. Coll. Int. Sci. **4**, 83 (1999).
- [40] K. Broderix, H. Löwe, P. Müller, and A. Zippelius, Phys. Rev. E **63**, 011510 (2001).
- [41] Y. Liu and R. B. Pandey, Phys. Rev. B **55**, 8257 (1997).
- [42] D. Vernon, M. Plischke, and B. Joós, Phys. Rev. E **64**, 031505 (2001).
- [43] M. Plischke, D. C. Vernon, and B. Joós, Phys. Rev. E **67**, 011401 (2003).
- [44] M. Wen, L. E. Scriven, and A. V. McCormick, Macromolecules **36**, 4151 (2003).
- [45] E. Del Gado, A. Fierro, L. de Arcangelis, and A. Coniglio, Europhys. Lett. **63**, 1 (2003).
- [46] I. Saika-Voivod, E. Zaccarelli, F. Sciortino, S. V. Buldyrev, and P. Tartaglia, Phys. Rev. E **70**, 041401 (2004).
- [47] J. C. Gimel, T. Nicolai, and D. Durand, Eur. Phys. J. E **5**, 415 (2001).
- [48] V. J. Anderson and H. N. W. Lekkerkerker, Nature **416**, 811 (2002).
- [49] E. Zaccarelli, F. Sciortino, S. V. Buldyrev, and P. Tartaglia, *Short-ranged attractive colloids: What is the gel state?*, pages 181–194, Elsevier, Amsterdam, 2004.
- [50] G. Foffi, C. De Michele, F. Sciortino, and P. Tartaglia, Phys. Rev. Lett. **94**, 078301 (2005).
- [51] E. Bianchi, E. Zaccarelli, F. Sciortino, and P. Tartaglia, in preparation (2005).
- [52] S. Sastry, Phys. Rev. Lett. **85**, 590 (2000).
- [53] S. Manley et al., Phys. Rev. Lett. **95**, 238302 (2005).
- [54] K. G. Soga, J. R. Melrose, and R. C. Ball, J. Chem. Phys. **110**, 2280 (1999).
- [55] J. F. M. Lodge and D. M. Heyes, J. Chem. Phys. **109**, 7567 (1998).
- [56] T. Vicsek, *Fractal Growth Phenomena*, World Scientific, Singapore, 1989.
- [57] M. Carpineti and M. Giglio, Phys. Rev. Lett. **68**, 3327 (1992).
- [58] F. Sciortino and P. Tartaglia, Phys. Rev. Lett. **74**, 282 (1995).
- [59] P. Poulin, J. Bibette, and D. A. Weitz, Eur. Phys. J. **7**, 277 (1999).
- [60] J. C. Gimel, T. Nicolai, and D. Durand, J. Sol-Gel Sci. Techn. **15**, 129 (1999).
- [61] F. Sciortino et al., Comp. Phys. Comm. **169**, 166 (2005).
- [62] A. Stradner et al., Nature **432**, 492 (2004).
- [63] A. I. Campbell, V. J. Anderson, J. van Duijneveldt, and P. Bartlett, Phys. Rev. Lett. **94**, 208301 (2005).
- [64] R. J. Speedy and P. G. Debenedetti, Mol. Phys. **81**, 237 (1994).
- [65] R. J. Speedy and P. G. Debenedetti, Mol. Phys. **88**, 1293 (1996).
- [66] Y. V. Kalyuzhnyi and P. T. Cummings, J. Chem. Phys. **118**, 6437 (2003).
- [67] M. S. Wertheim, J. Stat. Phys. **35**, 19 (1984).
- [68] A. Huerta and G. G. Naumis, Phys. Rev. B **66**, 1 (2002).
- [69] A. Huerta and G. G. Naumis, Phys. Lett. A **299**, 660 (2002).
- [70] M. H. Lamm, T. Chen, and S. C. Glotzer, NanoLetters **3**, 989 (2003).
- [71] K. van Workum and J. F. Douglas, Phys. Rev. E **71**, 031502 (2005).
- [72] J. Kolafa and I. Nezbeda, Mol. Phys. **61**, 161 (1987).
- [73] R. P. Sear, J. Chem. Phys. **111**, 4800 (1999).
- [74] N. Kern and D. Frenkel, J. Chem. Phys. **118**, 9882 (2003).
- [75] C. De Michele, S. Gabrielli, F. Sciortino, and P. Tartaglia, preprint condmat/0510787 (2005).
- [76] V. N. Manoharan, M. T. Elsesser, and D. J. Pine, Science **301**, 483 (2003).
- [77] A. Lomakin, N. Asherie, and G. B. Benedek, Proc. Natl. Acad. Sci. **96**, 9465 (1999).
- [78] R. Piazza, Curr. Op. Coll. Interf. Sci. **5**, 38 (2000).
- [79] G. Pellicane, D. Costa, and C. Caccamo, J. Phys.: Condens. Matter **15**, 375 (2003).
- [80] E. Zaccarelli, G. Foffi, F. Sciortino, and P. Tartaglia, Phys. Rev. Lett. **91**, 108301 (2003).
- [81] F. Sciortino, P. Tartaglia, and E. Zaccarelli, Phys. Rev.

- Lett. **91**, 268301 (2003).
- [82] T. Gleim, W. Kob, and K. Binder, Phys. Rev. Lett. **81**, 4404 (1998).
- [83] Y. Zhou, M. Karplus, J. M. Wichert, and C. K. Hall, J. Chem. Phys. **107**, 10691 (1997).
- [84] G. Foffi et al., Phys. Rev. Lett. **90**, 238301 (2003).
- [85] E. Zaccarelli et al., submitted (2006).
- [86] H. Tanaka, J. Meunier, and D. Bonn, Phys. Rev. E **69**, 031404 (2004).
- [87] A. J. Moreno et al., Phys. Rev. Lett. **95**, 157802 (2005).
- [88] M. Sperl, Phys. Rev. E **68**, 031405 (2003).
- [89] W. Götze and M. Sperl, Phys. Rev. E **66**, 011405 (2002).
- [90] L. Cipelletti, S. Manley, R. C. Ball, and D. A. Weitz, Phys. Rev. Lett. **84**, 2275 (2000).
- [91] E. Del Gado and W. Kob, (2005), preprint cond-mat/0510690.
- [92] S. Sastry, in preparation.
- [93] Of course, for convenience, in analogy to the definition of the glass transition, one can define a timescale above which the system is considered to be gelled, and use that as the definition of T_{gel} . In any case, independently of this definition, the gel line is rather flat.